Atmospheric plasma-based approaches for the degradation of dimethyl phthalate (DMP) in water

Kubra Ulucan-Altuntas[1,2], Mubbshir Saleem[1]*, Giulia Tomei[1], Ester Marotta[1]*, Cristina Paradisi[1]

[1] University of Padova, Department of Chemical Sciences, University of Padova, Via Marzolo 1, 35131 Padova, Italy

[2] Yildiz Technical University, Department of Environmental Engineering, Davutpasa, 34220, Istanbul, Turkey

*Corresponding authors

Ester Marotta,

Department of Chemical Sciences, University of Padova, Via Marzolo 1, 35131 Padova, Italy.

Email: ester.marotta@unipd.it

Mubbshir Saleem,

Department of Chemical Sciences, University of Padova, Via Marzolo 1, 35131 Padova, Italy.

Email: mubasher_sky@hotmail.com; mubbshir.saleem@unipd.it

Abstract

Cold plasma based treatment of contaminated water is gaining increasing attention as a novel green remediation option. This study assessed the performance of two different cold plasma reactors, using, respectively, a self-pulsing discharge (SPD) and a multipin corona discharge (MCD) in the degradation of dimethyl phthalate (DMP), a persistent and ubiquitous pollutant of the aquatic environment. The process kinetics and energy efficiencies, as well as the main plasma generated reactive species were determined under various operating conditions concerning the plasma feed gas, the voltage polarity, the input power, the DMP initial concentration, the liquid conductivity, and the aqueous matrix used to prepare DMP solutions for these experiments. The MCD reactor, operated with air as plasma feed gas and negative voltage polarity, gave the best energy efficiency. Further experiments with the MCD reactor demonstrated that plasma input power and initial liquid conductivity have limited effect on DMP degradation and, hence, on the reaction kinetics. This is a valuable feature, making this reactor suitable for treating liquids with a range of initial conductivities. It was also found that the initial concentration of DMP affects significantly both the rate of DMP degradation, which decreased with increasing concentration, and the process energy efficiency, which increased with increasing initial concentration. Interesting differences in the efficiency of production and distribution of plasma generated reactive species, notably $^{\bullet}OH$ and H_2O_2, were observed for the two tested reactors and are discussed in terms of different extension of the plasma/liquid interface and diffusion into the bulk solution. It is proposed that among the reactive species, $^{\bullet}OH$ foremost, and O_3 to a lesser extent, play a pivotal role in DMP degradation, while the contribution of H_2O_2 appears to be limited. The rate of DMP degradation was 2-times higher in ultrapure water than in tap water, a result attributed to the presence of the known hydroxyl radical scavengers' bicarbonate and carbonate.

Keywords:

Atmospheric plasma; self-pulsing discharge plasma; multipin corona discharge; dimethyl phthalate degradation; plasma treatment

1 Introduction

Phthalic acid esters (PAEs) have a multitude of industrial uses in the manufacture of paints, plastics (as plasticisers) and cosmetics, etc. (Ahmadi et al., 2020; Lee et al., 2019; Qi et al., 2019). These compounds are refractory and persistent, and can easily leach and accumulate in natural systems (water, soil, etc.) (Xu et al., 2020). Elevated concentrations of PAEs have been found in rivers (Zhao et al., 2020), ocean sediments (Hu et al., 2020), and soil samples (Jia et al., 2018; Moreno et al., 2020) across the world. Studies have reported that exposure to PAEs poses acute health risks to humans, including disruption in reproductive function, endocrine system disorders, and cancer (Hsu et al., 2016), even at low concentrations through accumulation in the food chain (Lyche et al., 2009). Due to these reasons, most PAEs are classified as priority pollutants by the United States Environmental Protection Agency (US EPA, 1991) and the European Union (European Union, 1993). Therefore, their treatment and removal are enforced by current regulations.

Biological treatment (Zhang et al., 2016), adsorption (Wang et al., 2010; Zhao et al., 2017), electrochemical and advanced oxidation processes (Li et al., 2020; Liu et al., 2019b, 2019a; Moreno et al., 2020) have been reported to eliminate PAEs from contaminated water efficiently. These technologies, however, have various shortcomings. Biological treatments are usually slow and require acclimatisation and enrichment of specific microorganisms, which are also sensitive to operational conditions (Li et al., 2017; Zhang et al., 2016). In adsorption, periodic regeneration or replacement of the adsorbents is needed with the consequent requirement for the management of secondary sources of contamination (i.e. the adsorbate) (Qi et al., 2019). Electrochemical and advanced oxidation/reduction processes have proven to be very effective in degrading PAEs in water; however, the use of additives and chemicals makes their application not very sustainable. Furthermore, the residues of these chemicals and additives in the treated water still pose a level of risk to the receiving environment (Qi et al., 2019). In this regard, atmospheric plasma discharges have been perceived as a more sustainable alternative to conventional AOPs. Among the benefits offered by atmospheric plasma treatment, its *in situ* generation of oxidising and reducing species

($^{\bullet}OH$, O, $O_2^{-\bullet}$, H, O_3, H_2O_2, aqueous and free electrons) without the input of any chemical or additive and its simple and flexible operation are the most appreciated and identify atmospheric plasma as a green technology (Foster, 2017).

Studies conducted in the past have reported efficient phthalates degradation using various gas phase (Jia et al., 2018; Kan et al., 2020; Qi et al., 2019) and liquid phase plasma discharges (Lee et al., 2019) in soil and water matrices. Furthermore, to enhance the energy efficiency of phthalates degradation using plasma treatment, the synergistic effect of various catalysts and added chemicals has also been investigated in hybrid plasma reactors (Ahmadi et al., 2020; Lee et al., 2019; Wang et al., 2018a). The plasma discharges tested in these studies generate specific reactive environments leading to different performances in treating the same phthalate compound, i.e. dimethyl phthalate (DMP). In this regard, Wang et al. (2018b) have reported a DMP degradation efficiency of 82.8% with an energy cost of 0.68 g/kWh using an air plasma diffused inside the liquid. In another study, the same group demonstrated the positive effect on DMP degradation associated with increasing input power frequency from 50 Hz (Wang et al., 2018b) to the kHz range (Kan et al., 2020). They achieved an energy yield (G_{50} value) of 1.35 mg/kJ, which is more than twice that (0.67 mg/kJ) obtained using the same reactor working in a hybrid mode system using sodium percarbonate at 50 Hz (Wang et al., 2018a). In another study, Qi et al. (2019) achieved up to 99.9% DMP removal with an energy efficiency of 0.2 g/kWh in a submerged microplasma jet array reactor. The authors reported an almost complete conversion of the parent contaminant into CO, CO_2, and H_2O and attributed this high degree of mineralisation and degradation efficiency to the efficient generation of OH radicals ($^{\bullet}OH$) and ozone (O_3). All these studies were performed using ultrapure water, whereas the water quality and purity in real contaminated samples are far worse. Since it is well known that the composition of the aqueous matrix can significantly influence the production and interaction of the reactive species generated by plasma, in this study, we treated DMP as an organic pollutant in tap water, chosen as a more realistic model for natural waters. We used a very efficient self-pulsing discharge (SPD) reactor, developed previously to treat surfactants like perfluorooctanoic acid

(PFOA) (Saleem et al., 2020). We also designed and developed a new plasma reactor based on a multipin corona discharge (MCD) concept (Miichi and Kanzawa, 2018) and compared its performance with the SPD reactor for DMP degradation. Initially, the effects of two major operating parameters were investigated, namely, the polarity of the applied voltage (negative and positive) and the plasma gas used (air and argon). Next, the better performing new MCD reactor was further tested to evaluate the effects of liquid conductivity, plasma input power, DMP initial concertation, and aqueous matrix (i.e. Milli-Q or tap water) on the process kinetics, on its energy efficiency, and on the production of major reactive species (i.e. $^{\bullet}OH$, O_3 and H_2O_2). The results provide a rationale for the significantly different performances of the two reactors under variety of conditions tested in this study.

2 Materials and methods

2.1 Chemicals and reagents

The synthetic solutions of dimethyl phthalate (DMP, Sigma Aldrich - reagent grade purity ≥ 99%) in concentration changing between 10^{-4} M - $2x10^{-6}$ M were prepared using tap water and Milli-Q water with initial conductivities of 480 and 4.5 μS/cm, respectively. Methanol (HPLC PLUS grade 99.9%) and sodium chloride (anhydrous ⩾ 99.5%) were purchased from Sigma-Aldrich. Dry Air and argon gases were purchased from Air Liquide with specified impurities detailed elsewhere (Saleem et al., 2020).

2.2 Plasma reactors and experimental procedure

Two types of plasma reactors were used in this work to treat DMP contaminated water. The first reactor, employing SPD plasma over the liquid surface, was used in a previous study in which it was efficient in degrading perfluorooctanoic acid (PFOA) (Saleem et al., 2020). In this study, the design of the SPD reactor was modified by introducing argon bubbling from the bottom of the reactor to improve the solution mixing. The second, the MCD (multipin corona discharge) plasma reactor, was purposely developed for this study. Each experiment was performed with 50 mL of

DMP solution in tap water at a constant input power. The first series of batch experiments were performed to assess the plasma reactor performance in degrading DMP solution (2×10^{-5} M) using air or argon as plasma feed gas and applying negative and positive polarity of the high voltage power supply. Afterwards, the better performing reactor working under its most suitable operating conditions was further tested in successive experiments to investigate the effects of initial DMP concentration, liquid conductivity, plasma input power, and the aqueous matrix (i.e. Milli-Q or tap water) on DMP degradation efficiency. The reactors were supplied with pre-humidified gas (air or argon) to avoid water evaporation from the treated solution.

Similarly, before switching on plasma discharge, the reactors were always flushed for 1–2 min with plasma feed gas (synthetic air or argon) to be used in the experiment at a flow rate of 400 mL/min. The effect of liquid conductivity was studied by adding NaCl in Milli-Q and tap water and by concentrating tap water through evaporation at 60 °C and adjusting conductivities to 1000 µS/cm and 2000 µS/cm to mimic actual groundwater conditions. First experiments were repeated three times to test the overall reproducibility of the obtained results with both the reactors, and it was within 10%. Considering that the experiments were carried out in batch modality and thus each datum of a series is obtained in an independent experiment, the following plasma treatments were repeated under the same conditions only if the obtained result was inconsistent with the other data of the series.

2.2.1. Self-pulsing discharge (SPD) reactor

The reactor consisted of a Pyrex cylinder with 43 mm internal diameter and 3 mm thickness having a total volume of 120 mL (Fig. 1a). The cylinder was closed at the top with a Plexiglas cover fitted with a nitrile rubber O ring to make it airtight. The cover was provided with ports for the gas outlet, sample collection, and integration of the high voltage electrode. A pointed edge high voltage electrode made of tungsten (2 mm in diameter) was placed 4 mm above the liquid surface. The ring-shaped grounded electrode (43 mm in diameter) was made from a 1 mm thick stainless-steel wire

and placed 10 mm below the surface of the liquid (Fig. 1a) (Saleem et al., 2020). Plasma gas (argon or air) was supplied at a flow rate of 100 mL/min through a ceramic gas diffuser fitted at the bottom of the SPD reactor covering the entire base of the Pyrex cylinder. Gas bubbling through the diffuser also ensured uniform mixing of the liquid sample to be treated during the experiment.

2.2.2. Multipin corona discharge (MCD) reactor

For the MCD reactor, the same airtight Pyrex reactor was used. The high voltage electrode was made of a 4 mm diameter hollow stainless-steel rod placed along the axis of the reactor (Fig. 1b). The end of the hollow electrode was fitted with an aluminium disc (35 mm in diameter and 2 mm thick) containing 32 evenly distributed 5 mm long stainless steel pins and a central hole 1 mm in diameter for the gas supply. The edge of the multipin electrode was placed at a desired distance above the liquid surface to control the discharge voltage and hence, the plasma input power. A grounded electrode (a steel wire with 1 mm diameter) was placed at the bottom of the reactor 20 mm below the liquid surface (Fig. 1b). Plasma gas (argon or air) was supplied at a flow rate of 100 mL/min through the hollow electrode. Continuous mixing of the solution was provided by placing the reactor over a magnetic stirrer.

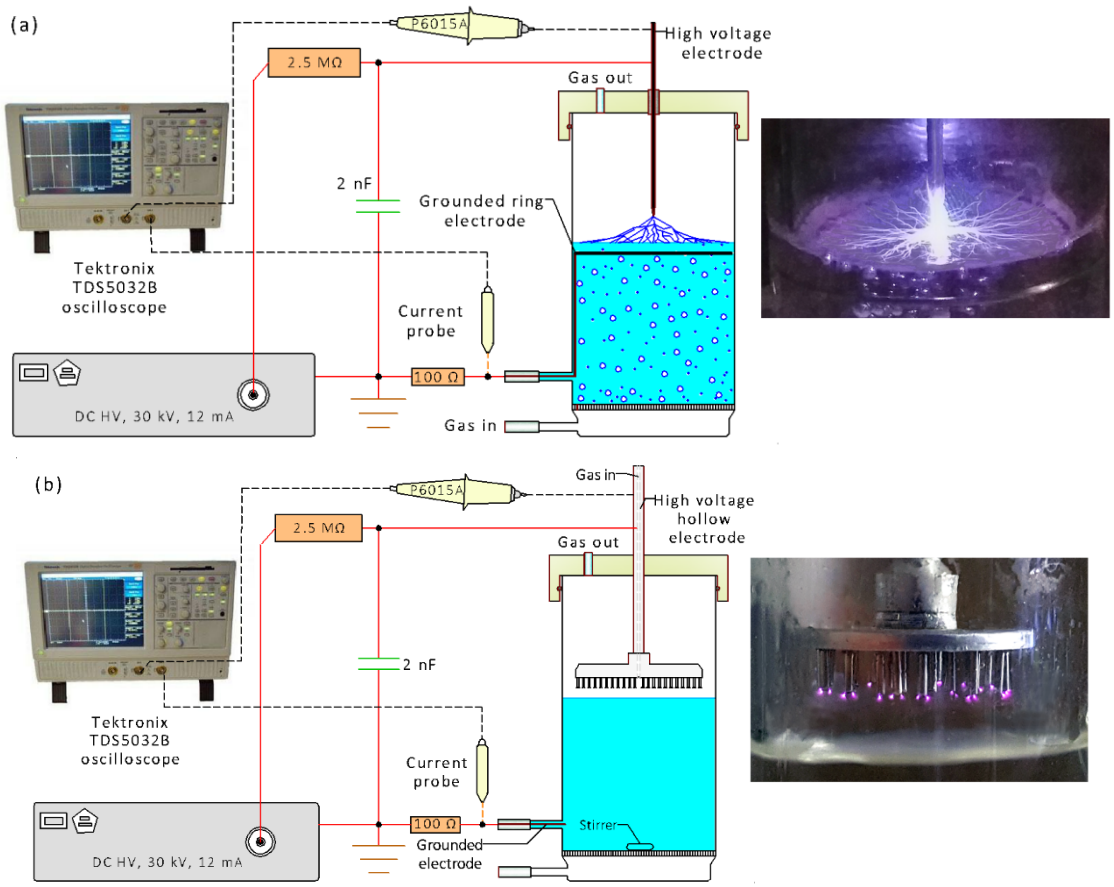

Figure 1 Schematic representation of the experimental setups (figure not to scale) and the actual photographs of the two discharges with negative voltage polarity (a) SPD reactor and (b) MCD reactor.

2.3. Power supply characteristics and electrical measurements

In both cases, plasma was ignited with a Spellman PTV30*350 (30 kV, 12 mA) high voltage power supply with negative and positive polarity and protected by a 2.5 MΩ high voltage resistor (Fig. 1). Plasma was generated by charging a high voltage capacitor (2 nF) connected in parallel to the SPD and MCD reactors (Fig. 1). As described in the previous publication (Saleem et al., 2020), the SPD reactor acted similarly as a spark gap where the capacitor is charged up to the breakdown voltage, and the discharge is distributed to numerous leaders and streamers upon striking the liquid surface (Fig. 1a). Therefore, the deposited charge of the capacitor determined the energy of the single pulse (E_p) in the SPD regime and was calculated using the following formula

$$E_p = \frac{CV^2}{2} \quad (1)$$

where C is the capacitance and V is the applied voltage. The energy of the single pulse was also measured by integrating the pulse power over time using the equation ($E_{pulse} = \int_0^\tau u(t) \cdot i(t) \cdot dt$). The measurements confirmed the validity of the pulse energy determination using Eq. 1, and the accuracy of the used method was within 2%. Since the breakdown voltage in the SPD reactor depends on the type of plasma gas (air or argon) and the conductivity of the treated solution, it varied between 5.8-6.2 kV under the combination of various operating conditions. Thus, constant input power to the SPD discharge was controlled by regulating the capacitor charging current from the power supply within the frequency range of 60-100 Hz. The working mechanism of the SPD plasma and characteristics of the voltage and current waveforms are presented and discussed in details elsewhere (Saleem et al., 2020; Sretenović et al., 2021). In the corona regime, the formation of pulse discharge and thus, the electrical breakdown was controlled by limiting the current supplied to the high voltage capacitor. Therefore, the discharge appears localised near the sharp edges of the multipin electrode as shown in Fig. 1b.

The voltage was measured using a high voltage probe, Tekronix P6015A connected to a Tekronix TDS5032B oscilloscope (350 MHz, 5 GS/s), while the current was measured by determining the voltage drop across the non-inductive resistor mounted between the ground electrode and the grounding point, using an ordinary voltage probe for both the reactors. The average powers of each treatment interval were multiplied by the duration of intervals (i.e. 5 min) to determine the consumed energies. The average consumed energies of each treatment were added and divided by the total treatment time. Thus, the average powers for the complete treatments were determined. In the case of the SPD reactor, the average power delivered to the plasma was kept constant by controlling the discharge frequency. In the case of the MCD reactor, the voltage and current values were recorded every 5 minutes, and the instantaneous power was simply calculated as the product of the measured values. The average power over the whole duration of plasma treatment (T) was then calculated using the following equation (Ceriani et al., 2018).

$$\bar{P} = \frac{\sum P(t) \cdot \Delta t}{T} \quad (2)$$

where Δt is the time interval between two consecutive readings and ∑ P(t) is the sum of instantaneous power measurements.

2.4. Analytical procedures

The residual DMP concentration after each treatment in one of the plasma reactors was measured as a function of treatment time and energy applied using an HPLC system (Agilent Technologies 1260 series) connected to a UV detector G7114A VWD. The chromatographic separation was performed using a Phenomenex Kinetex 5 µm C18 column (100 Å, 150 × 4.6 mm). The eluents used consist of Milli-Q water (A) and methanol (B). The gradient for eluent B was as follows: from 10% to 50% in 11 min, from 50% to 100% in 7 min. The flow rate was set at 1.0 mL/min, and the injection volume was 20 µL. The elution was followed at 228 nm. The quantification of DMP was based on an external calibration curve.

The residual DMP concentrations determined by the HPLC system were interpolated with a first-order decay exponential function versus time (Eq. 3) to obtain *k* the process pseudo-first rate constant according to the kinetic scheme described elsewhere (Marotta et al., 2011).

$$C = C_0 \cdot \exp(-k \cdot t) \quad (3)$$

The extent of DMP conversion was estimated according to Eq. 4.

$$\%\ DMP\ conversion = 100 \cdot \frac{C_0 - C_t}{C_0} \quad (4)$$

where C_0 and C_t are the DMP concentrations before the treatment and after treatment of duration t, respectively.

The solution conductivity was measured using a Metrohm 660 Conductometer equipped with a 6.0901.130 electrode. The energy yield for the reactors, G_{50}, defined as the amount of DMP degraded per kWh of energy consumed to achieve 50% conversion, was calculated using Eq. 5 (Arif Malik, n.d.)

$$G_{50}(mg/kWh) = \frac{1.8 \cdot 10^9 \times C_0(mol/L) \times V(L) \times MM(g/mol)}{P(W) \times t_{1/2}(s)} \quad (5)$$

where C_0 represents the initial DMP concentration, V is the treated volume, MM is the molar mass of the pollutant, P is the mean power of the reactor, and $t_{1/2}$ is the time required for the pollutant to achieve 50% conversion.

We attempted to determine the ozone concentration in plasma-treated aqueous solutions using the Indigo method (Bader and Hoigné, 1981). However, these analyses showed problems connected to the fact that in plasma-activated waters (PAWs), Indigo can also react with other species, such as •OH, so it was not selective for ozone (Tarabova et al., 2018). Therefore, we resorted to determine the ozone concentration in the gas phase, using the MCD reactor and comparing the amounts of ozone released in tap water treatment with and without DMP ($2x10^{-5}$ M). The procedure for determining ozone by the iodometric titration method was previously mentioned in the article (Marotta et al., 2011). The gas in the outlet of the reactor was connected to two bubblers in sequence, each containing 150 mL of 0.12 M KI solution in phosphate buffer. After each experiment, the two KI solutions were combined, acidified with 5 mL of 4.5 M H_2SO_4, and titrated with a standardised 0.1 M thiosulfate solution.

The hydrogen peroxide concentration in the liquid phase during the treatment was determined by the titanium oxysulfate assay described elsewhere (Eisenberg, 1943). 0.12 mL of titanium oxysulfate was added to 3 mL of plasma-treated tap water after the addition of 0.6 mL of 0.3 M sodium azide solution in order to prevent hydrogen peroxide decomposition by NO_2^- under acidic conditions (Lukes et al., 2014; Tarabova et al., 2018). The UV-Vis absorption analysis of samples was carried out with a Varian Cary100 spectrophotometer (λ (absorption) = 420 nm).

The quantitative determination of •OH formation rate was based on the treatment of 1 mM disodium terephthalate solution in tap water (Sahni and Locke, 2006). The parent compound degradation and the fluorescent product formation resulting from the terephthalate reaction with •OH (2-hydroxyterephthalate) were detected. The quantification of the compounds was based on an external

calibration curve. For the determination of •OH in the SPD reactor using argon, 0.33 mM K_2IrCl_6 was added to the disodium terephthalate solution before the treatment to have an oxidant, $IrCl_6^{2-}$, which promotes the formation of 2-hydroxyterephthalate after the addition of •OH to the aromatic ring of the terephthalate anion (Mark et al., 1998).

The degradation of disodium terephthalate was monitored using the same HPLC-UV system described above. The chromatographic separation was performed using a Phenomenex Kinetex 5 µm C18 column (100 Å, 150 × 4.6 mm). The eluents used consist of Milli-Q water + 0.1% formic acid (A) and acetonitrile + 0.1% formic acid (B). The gradient for eluent B was as follows: from 10% to 38% in 7 min, from 38% to 100% in 5 min. The flow rate was set at 1.0 mL/min, and the injection volume was 5 µL. The elution was followed at 232 nm. The 2-hydroxyterephthalate was analyzed with a Perkin Elmer LS-55 fluorimeter (λ(excitation) = 315 nm; λ(emission) = 425 nm). The concentration of 2-hydroxyterephthalate in solution after the treatment was correlated to the •OH formation rate using Eq. (6)

$$V_{[\cdot OH]}\ (M/min) = \frac{V_{[2OH-t]}}{yield\ of\ the\ reaction} \quad (6)$$

where $V_{[2OH-t]}$ represents the slope of the line obtained by fitting the concentration of 2-hydroxyterephthalate as a function of treatment time, while the yield of the reaction is 35% in air (MCD) and 85% in argon (SPD) (Mark et al., 1998). Alkalinity analysis was performed according to Standard Methods 2320 (APHA, AWWA, 2012).

3. Results and discussion

3.1. Comparative performance evaluation of SPD and MCD reactors in DMP degradation

The type of discharge used greatly influences the reactive environment within the generated plasma and thus affects the degradation efficiency of contaminants exposed to its action (Jiang et al., 2014; Saleem et al., 2020). Therefore, the first phase of the study was focused on testing and comparing the two plasma reactors selected for this study, namely the SPD reactor, which was available from

previous work on PFAS treatment, and the MCD reactor, which was developed here for the treatment of non-surfactant pollutants, such as DMP. These comparative tests evaluated the effects of plasma feed gas (air or argon) and the high voltage polarity. For this purpose, 50 mL of $2x10^{-5}$ M DMP solution in tap water was treated using the two reactors for 15 min at a constant power input of 1.5 W (Fig. 2a). The low input power of 1.5 W was selected because at higher power (i.e. at higher applied voltage) the corona discharge could develop into SPD under argon atmosphere. The results of these experiments are summarised in Fig. 2. It is evident from Fig. 2a that for the MCD reactor, the highest DMP degradation (up to 60% in a 15 min treatment) was achieved using air atmosphere and negative polarity, whereas way more limited degradation (30%) was achieved with an argon atmosphere. The limited production of useful oxidising reactive species in an argon plasma (i.e. $^{\bullet}OH$ and H_2O_2, with no production at all of O_3) (Du et al., 2008) renders its use inefficient for DMP degradation in the MCD reactor indeed. The corona discharge under argon atmosphere produces metastable argon species, including Ar^+ (Yang et al., 2013), which is known to be a strong oxidant (Stratton et al., 2017). In contrast with the MCD reactor, the SPD reactor was more efficient under argon than under air atmosphere and with positive polarity achieved DMP degradation up to 45%. However, it should be noted that the voltage polarity is not so significant for the SPD reactor under argon atmosphere. In the previous study performed with the same type of discharge as that in the SPD reactor used here, we observed a similar effect, the degradation of PFOA being higher with argon than with air (Saleem et al., 2020). We had attributed the more unsatisfactory performance of the discharge in air to the increase in the solution conductivity due to air plasma generated nitrous and nitric acids, leading to a less efficient spreading of the discharge streamers over the liquid surface and thus to a reduced plasma-liquid interface. When argon is used to feed the discharge, no NO_x is produced, and no significant changes occur in the liquid conductivity. However, in the case of DMP degradation, the efficiency of SPD in Ar is relatively low even at higher input power, as shown in Figure 2b, in which a $2x10^{-5}$ M DMP solution was treated at a constant power input of 6 W.

The effect of the applied voltage polarity on DMP degradation in the MCD reactor was further investigated in a separate set of experiments in which 50 mL of $2x10^{-5}$ M DMP solution in tap water were treated at a constant power input of 3 W (Fig. 2c). DMP degradation was higher using –ve polarity, i.e. 91%, whereas it was only 60% for the positive polarity in 30 min of treatment. The observed k values were 0.080 and 0.032 min^{-1} for negative and positive polarity, respectively. Similarly, the calculated G_{50} value for the experiment using –ve polarity was approximately 2.5 times higher as compared to that with positive polarity. In negative polarity, high energy electrons and negative ions move away from the active electrode (in this case the multipin electrode) towards the liquid surface (i.e. acting as an opposite electrode) due to which formation and diffusion of the reactive species is enhanced and consequently contaminant degradation is promoted (in this case DMP) (Nani et al., 2018).

a.

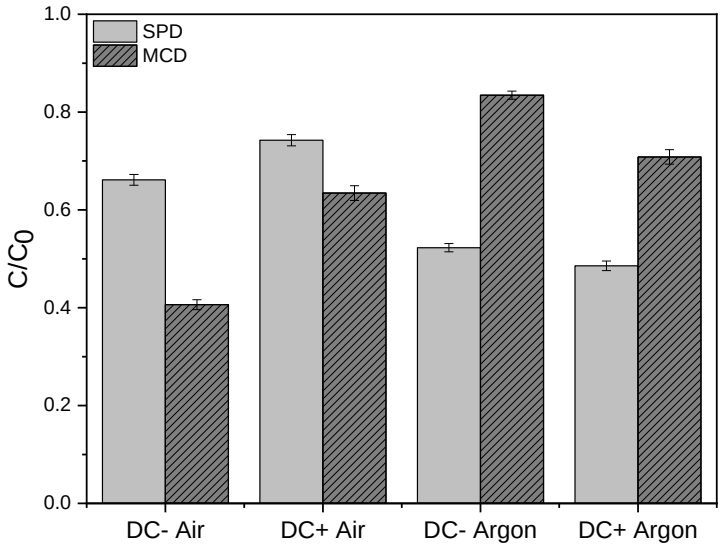

b.

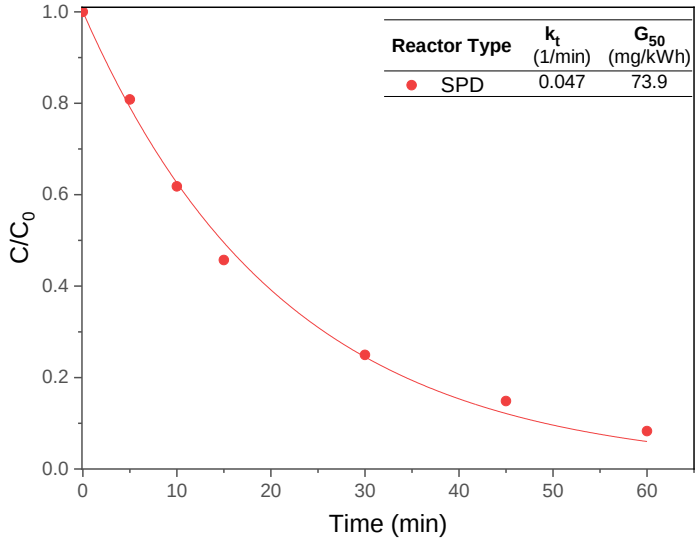

c.

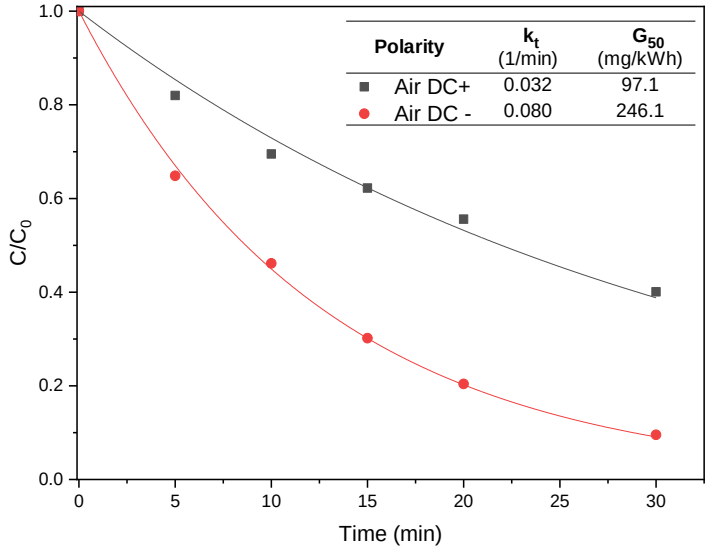

Figure 2 (a) Effect of the type of plasma discharge and operating parameters (i.e. voltage polarity and plasma gas) on DMP degradation efficiency (input power = 1.5 W, treatment time = 15 min) **(b)** Degradation of DMP as a function of time using the SPD reactor (C_0 = 2x10^{-5} M, DC +, P = 6 W and argon) **(c)** Effect of voltage polarity (i.e. negative/positive) on DMP degradation as a function of treatment time using the MCD reactor (C_0 = 2x10^{-5} M, P = 3 W and air).

As stated earlier, it is known that the type of plasma discharge greatly influences the generation of the reactive species ($^{\bullet}$OH, O_3, and H_2O_2, etc.). Therefore, the marked difference in the performance of the two tested reactors and thus in the obtained G_{50} values is to be attributed to the different distributions and amounts of useful reactive species produced in the two setups. Fig. 3a and 3b report on the production of $^{\bullet}$OH and H_2O_2, respectively, in tap water treated in the two reactors, SPD and MCD, operated at a constant input power of 3 W, without the addition of DMP. It is seen

that the concentration of 2-hydroxyterephthalate, which is correlated to the presence of •OH in the solution, increased steadily in both reactors: after 15 minutes of treatment, it was 13 µM and 16 µM in the SPD and MCD reactors, respectively (Fig. 3a). The rate of •OH generation, determined from these data, was 3.1 µM/min in the MCD reactor, which is almost 3 times higher than that in the SPD reactor (i.e. 1.1 µM/min). However, the production of H_2O_2 was significantly higher in the SPD reactor than the MCD reactor (Fig. 3b). The maximum concentration of H_2O_2 achieved after 30 min of plasma treatment in the SPD reactor reached up to 730 µM, which is 6 times higher than the corresponding data obtained in the MCD reactor. Since •OH is mainly formed from the dissociation of water (Eq. 7) and H_2O_2 mainly originates from •OH recombination (Eq. 8), hydrogen peroxide is often considered to be a reasonable indicator for hydroxyl radical formation in plasma in contact with water (Locke and Shih, 2011). However, this correlation does not appear to be holding for the experiments using the SPD reactor since the •OH formation rate is similar to that measured in the MCD reactor, whereas the concentration of H_2O_2 detected in the SPD is far higher than in the MCD reactor (Fig. 3b). These results can be explained considering that the ratio between •OH and H_2O_2 depends on several factors, including the presence of other chemical species contributing either to the formation or to the destruction of •OH and H_2O_2 (see for example Eq. 9, which is not expected to take place in the SPD reactor under argon atmosphere), as well as the input power, including current and voltage waveforms, plasma characteristics and gas-liquid interfacial contact patterns (Locke and Shih, 2011). It is known that SPD produces significant amounts of high-energy electrons in argon atmosphere (Mededovic Thagard et al., 2017; Saleem et al., 2020), which react at the liquid surface inducing water dissociation (Eq. 7) thus forming •OH radicals. It is, therefore, reasonable to expect that the •OH production rate is significantly higher than that measured with the disodium terephthalate probe in the bulk solution, because of the occurrence of efficient •OH recombination (Eq. 8) which limits radical diffusion into the liquid. The •OH formation rate measured through the disodium terephthalate probe is thus to be considered a lower limit, as the probe only detects the fraction of the •OH available for reacting within the bulk

solution, while electrons do not seem able to diffuse in the bulk and promote the back dissociation of H_2O_2 into $^{\bullet}OH$ (Eq. 10).

$$H_2O + e^- \rightarrow {}^{\bullet}H + {}^{\bullet}OH + e^- \quad (7)$$

$$^{\bullet}OH + {}^{\bullet}OH \rightarrow H_2O_2 \quad (8)$$

$$H_2O_2 + O_3 \rightarrow {}^{\bullet}O_2H + {}^{\bullet}OH + O_2 \quad (9)$$

$$H_2O_2 + e^- \rightarrow {}^{\bullet}OH + {}^{\bullet}OH + e^- \quad (10)$$

This is also the fraction of $^{\bullet}OH$ which is available for the reaction with organic contaminants dissolved into the bulk of the solution. Unlike the SPD reactor, the discharge in the MCD reactor was localised near the edges of the multipin electrode (Fig. 1b) and not touching the liquid surface; therefore, loss of $^{\bullet}OH$ due to its recombination (Eq. 8) in comparison to its production in the MCD reactor was less important. Comparing the SPD and MCD reactors, the degradation of dissolved pollutants will be favoured in the MCD reactor because of the slightly higher production of $^{\bullet}OH$ available in the liquid. On the contrary, to efficiently react with organic compounds, H_2O_2 would need to be activated. For example, H_2O_2 has shown to play a pivotal role by enhancing DMP degradation through a synergistic effect in hybrid plasma treatment systems using sodium percarbonate (Wang et al., 2018a) or heterogeneous catalysts (i.e. α-Fe_2O_3-TiO_2 - (Ahmadi et al., 2020)). Likewise, Wang et al. (2018a) also suggested that H_2O_2 participated in the DMP degradation process via indirect oxidation through the production of $^{\bullet}OH$ activated by the action of ultraviolet (UV) irradiation, high-energy electrons (Eq. 10) or reaction with ozone (Eq. 9).

a.

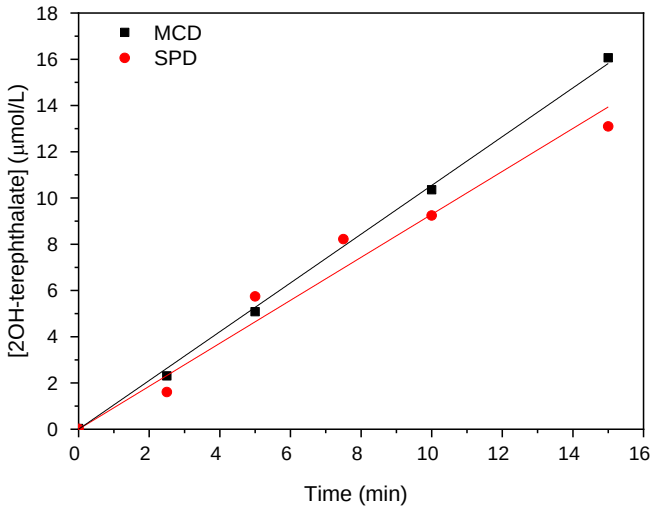

b.

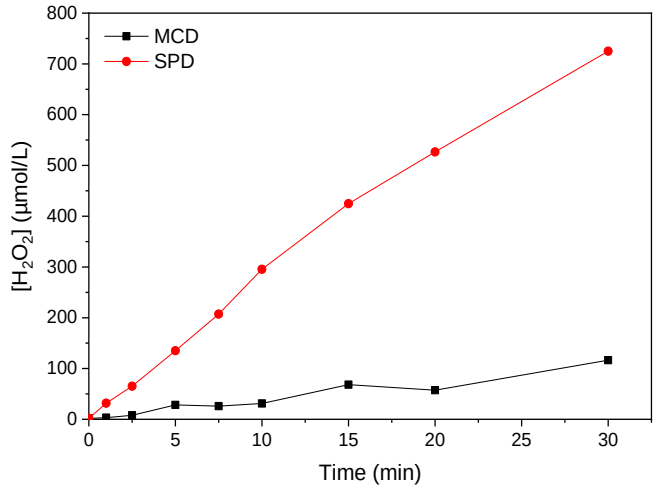

c.

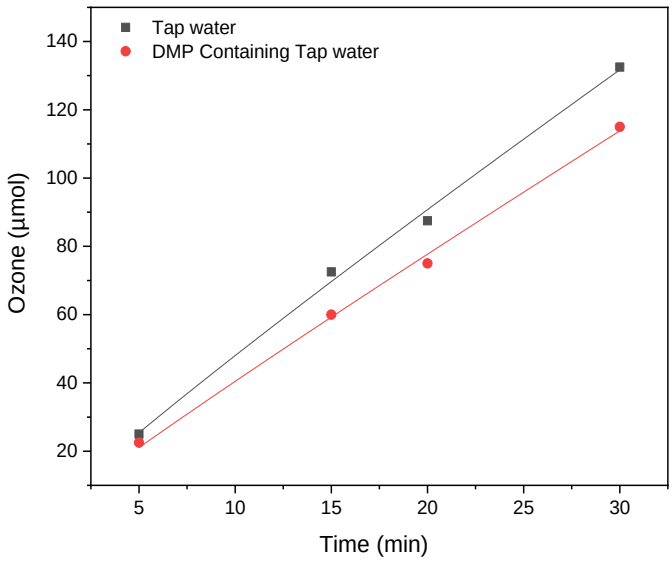

Figure 3 Experimental results used for the determination of reactive species during treatment of tap water in the SPD (P = 3 W, DCpositive and argon) and MCD (P = 3 W, DC negative and air) reactors: **(a)** concentration of 2-hydroxyterephthalate used for determination of •OH rate of formation by Eq. (6), **(b)** concentration of hydrogen peroxide and **(c)** amount of ozone in the gas sampled at the reactor's outlet during the treatment of tap water (black square symbols) and of a $2x10^{-5}$ M DMP solution in tap water (red dot symbols) in the MCD reactor.

Fig. 3c represents the amount of ozone measured in the gas escaping the MCD reactor during air plasma treatment of tap water with and without dissolved DMP (C_0 = 2x10^{-5} M). Not surprisingly, analogous experiments carried out with the SPD reactor operated under its optimal conditions, notably with argon instead of air as the plasma feed gas, failed to detect any ozone in the outlet gas. Shiraki et al. (2016), in a similar pulsing discharge plasma reactor in contact with liquid under argon atmosphere, reported a trend similar to ours for H_2O_2 production and mentioned that the concentration of O_3 in the gas phase was negligible and was lower than the minimum detection limit. The amount of O_3 in the MCD reactor reached the highest values of 133 µmol and 115 µmol after 30 min plasma treatment of tap water and DMP solution, respectively (Fig. 3c). The slight decrease in the amount of O_3 (around 14%) observed in the presence of DMP is attributed to the ozone consumption in possible reactions with DMP itself and with its degradation by-products in the treated solution. This observation is particularly critical when considering the efficient design of a plasma reactor and implies that even though the MCD reactor performed better than the SPD reactor in DMP degradation, a large quantity of O_3 was wasted that should instead be utilised in the process. This could be done by recycling and bubbling the exhaust gas containing ozone into the same reactor or into the tank containing the solution to be treated, as proposed by Wang et al. (2020). This comparative investigation thus indicates that H_2O_2 has a limited role in DMP degradation using plasma alone under the conditions studied in this work, whereas $^{\bullet}OH$ foremost, and O_3 to a lesser degree, play a more significant role. Considering the previous literature concerning treatment of DMP, this is consistent with a study in which Liu et al. (2019b) have found enhanced DMP degradation when ozonation was performed over nanostructured Cu-Fe-O as compared to the O_3 alone process and have attributed this result to the much more efficient generation of $^{\bullet}OH$ in the catalyst assisted reaction.

3.2. DMP degradation efficiency in the MCD reactor: effect of operation parameters

This section presents an account of the effects of plasma input power and initial liquid conductivity on the kinetics and energy efficiency of DMP degradation process using the better performing reactor evaluated in the previous section (i.e. the MCD reactor).

3.2.1. Effect of plasma input power

The input power supplied to the plasma is an important operating parameter as it is directly proportional to the degree of gas ionisation, and it governs the generation of reactive species that in turn determine k and G_{50} values (Kan et al., 2020). The effect of applied power on DMP degradation was evaluated using the negative polarity under air atmosphere while treating 50 mL of $2x10^{-5}$ M DMP solution. Due to the transformation of corona discharge into SPD regime at high input power, the effect of input power was only investigated within the 1.5 – 4 W range maintaining a fixed distance of 4 mm between the liquid surface and the multipin electrode. The results of DMP degradation and the corresponding G_{50} values are presented in Fig 4a. The DMP degradation profiles are well-correlated with first-order kinetics, with the calculated k values increasing by almost 30% from the value obtained at 1.5 W (0.063 min^{-1}) to that at 3 W (0.080 min^{-1}) and remaining almost constant with a further increase of the power to 4 W. The highest G_{50} value (393 mg/kWh) was observed for 1.5 W input power which thus appears to be the most suitable condition from the viewpoint of energy efficiency for DMP degradation in the MCD reactor. Qi et al. (2019) have also reported a similar observation for a microplasma array reactor for which, after reaching a certain power level, any further increase in power did not produce any significant effect on DMP degradation efficiency. To gain insight into this phenomenon, we investigated the production of $^{\bullet}OH$, the most important reactive species in DMP degradation described in section 3.1, as a function of input power within the 1.5 W – 4 W range. The experimentally determined rates of $^{\bullet}OH$ generation were 2.3 µM/min, 3.0 µM/min, and 2.2 µM/min for 1.5, 3, and 4 W plasma input power, respectively (Fig. 4b). The generation rate of $^{\bullet}OH$ at 3 W of plasma input power was approximately 1.3 times higher than found at both 1.5 W and 4 W. This difference appears to reflect in the slightly

higher DMP degradation efficiency (Fig. 4a) and k value for treatment at 3 W as compared to those determined at both 1.5 and 4 W. In contrast with our observations, an increase in the input power for plasma generation has often been found to produce a concomitant increase in the production of •OH via water dissociation (Locke and Shih, 2011). An example dealing with the degradation of DMP was given by Wang et al. (2018b) for a submerged surface discharge plasma reactor. These different behaviours can be explained by the different balances established under different power input conditions, between •OH-forming and •OH-consuming reactions, including notably recombination (Eq. 8). The match of the highest degradation efficiency with the highest rate of formation of •OH observed in the MCD reactor allows us to confirm the important role of •OH in the degradation process of DMP.

a.

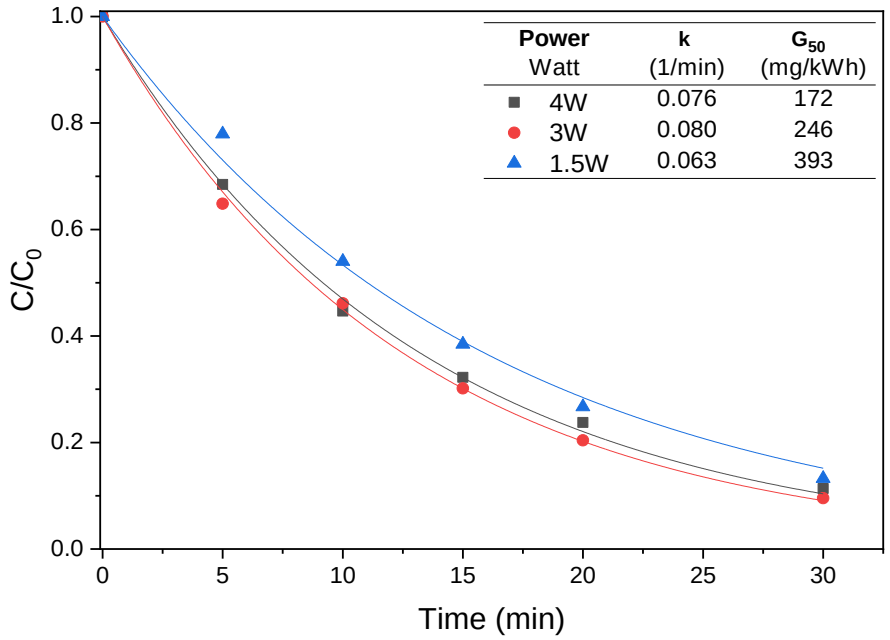

b.

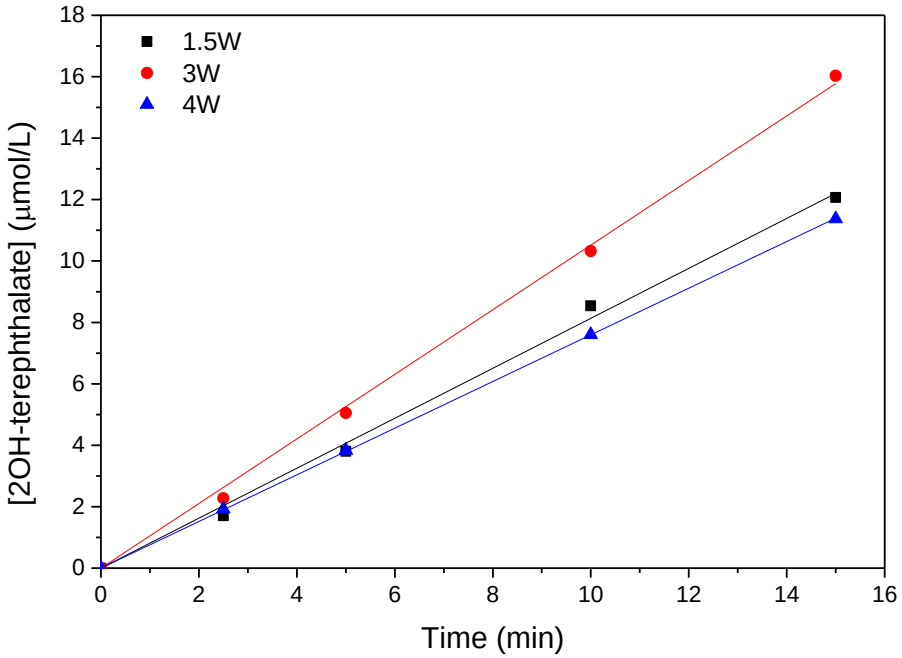

Figure 4 Effect of plasma input power, using the MCD reactor, on **(a)** the DMP degradation efficiency as a function of time (C_0 = 2x10^{-5} M, DCnegative and air) and **(b)** the generation of •OH in tap water (DCnegative and air).

3.2.2. Effect of initial DMP concentration and the aqueous matrix

The effect of the initial DMP concentration on the degradation efficiency and the corresponding G_{50} value is presented in Fig. 5. It can be seen that the degradation efficiency correlates inversely with the initial DMP concentration. As a result, in 30 min treatment time, the extent of DMP removal decreased from virtually complete, when used at the lowest tested concentration (2x10^{-6} M), to 91% and 61% when used at initial concentrations of 2x10^{-5} M and 1x10^{-4} M, respectively. The associated k values increased correspondingly, the largest k value (0.096 min^{-1}) being observed for degradation of DMP at the lowest initial concentration tested, 2x10^{-6} M (Fig. 5). Similar relationships among the initial pollutant concentration, its degradation efficiency, and the corresponding k value have been reported in previous studies on plasma-induced degradation of organic contaminants (Bosi et al., 2018; Krishna et al., 2016; Tampieri et al., 2018), and, in particular, of DMP (Kan et al., 2020; Wang et al., 2018b). They have been attributed to 1) the effect of the initial pollutant concentration on the molar ratio between the reactive species and the pollutant itself (the lower its initial concentration, the higher the relative amount of reactive species available to react with it and thus the rate of its degradation) (Kan et al., 2020; Krishna et al., 2016; Wang et al., 2018b) and 2) to

inhibition of the pollutant reactions due to competing reactions of available reactive species with the organic intermediates formed in the degradation of the pollutant itself (the higher its initial concentration, the higher that of its intermediates and thus the more efficient their competition for the plasma generated reactive species) (Bosi et al., 2018; Krishna et al., 2016; Slater and Douglas-Hamilton, 1981; Tampieri et al., 2018). In our study, although the highest k value was observed at a low initial concentration of $2x10^{-6}$ M with complete DMP degradation, the highest G_{50} value of 537 mg/kWh was found at an initial concentration of $1x10^{-4}$ M with a relatively moderate degradation extent of around 61% (Fig. 5). Qi et al. (2019) obtained up to 68.8% DMP degradation in a microplasma array reactor by applying 4.7 W input power for an initial DMP concentration of 30 mg/L in 60 min treatment. Observing these data, one can estimate a G_{50} value of approximately 322 mg/kWh which is lower than the value reported in this study (i.e. 537 mg/kWh). Very high G_{50} values were instead obtained in two recent studies using submerged surface discharge plasma reactor for the degradation of DMP. Wang et al. (2018b) obtained an estimated G_{50} value of 1040.8 mg/kWh at a frequency of 50 Hz, while Kan et al. (2020) reported a G_{50} value of 4860 mg/kWh (1.35 mg k/J) operating at 7 kHz, both significantly greater than the values obtained in this study. However, in these studies, deionised water was used in contrast with the work reported here, mainly performed using tap water to simulate realistic conditions. Therefore, in order to evaluate the effect of the aqueous matrix (Milli-Q or tap water) on DMP degradation, a set of experiments was performed in Milli-Q water with DMP at an initial concentration of $2x10^{-5}$ M. The k value determined in these experiments was the highest observed in this study, allowing to achieve up to 97% DMP degradation in 15 min with a G_{50} value about doubled with respect to the use of tap water (Fig. 5).

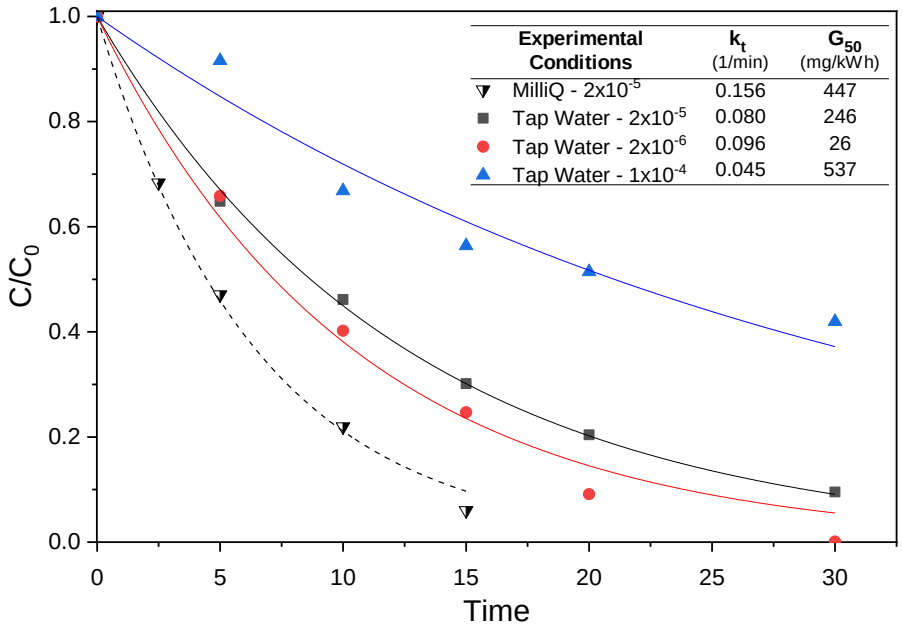

Figure 5 Effect of initial concentration and aqueous matrix on DMP degradation efficiency as a function of time (P = 3 W, DCnegative, and air).

3.2.3. Effect of initial liquid conductivity

The impact of the solution conductivity on DMP degradation performance was investigated by preparing 2x10^{-5} M DMP solutions in Milli-Q and tap water and by treating them in the MCD reactor at a constant power input of 3 W. As shown in Fig. 6a, the degradation efficiency of DMP in Milli-Q water does not appear to be affected significantly by the changes in the solution conductivity within the tested range in this study (i.e. 4-1000 µS/cm). Besides, the rise in the solution's conductivity after the treatment was also not too high (Table 1). Likewise, when the conductivity of tap water was increased from 450 to 1000 µS/cm by adding NaCl, the difference in DMP degradation efficiency was almost insignificant and approximated to be only 4% (Fig. 6a) with slight differences in the calculated k and G_{50} values of around 8% and 14%, respectively (Fig. 6b). These observations imply that the operation and stability of the MCD reactor were not affected by the initial conductivity of the solution. This feature is particularly advantageous compared to the performance of those electrical discharge plasma systems whose performances are highly dependent on the solution conductivity, such as the SPD reactor used in this study (Saleem et al., 2020).

On the contrary, the DMP degradation efficiency progressively decreased with increasing liquid conductivity in experiments performed with concentrated tap water samples obtained after water evaporation (Fig. 6a). When the conductivity was raised to 1000 µS/cm and 2000 µS/cm, the DMP degradation decreased to 72% and 58%, respectively, of the degradation obtained in the non-concentrated tap water sample. Similarly, the calculated k and G_{50} values for the concentrated tap water sample with a conductivity of 1000 µS/cm was at least 1.7 and 1.8 times lower than the corresponding values determined in tap water (Fig. 6b). Considering the strong influence that pH can have on the distribution and solubility of relevant reactive species (Attri et al., 2015; Marotta et al., 2012), the pH values of the samples before and after plasma treatment were monitored in all performed experiments and are reported in Table 1. It can be observed that, while in Milli-Q water the pH decreases during the treatment due to the production of nitric acid, which typically occurs in water treated with a plasma produced in air and was detected by ion chromatographic analyses, in tap water, the presence of the bicarbonate/carbonate system provides a buffering effect which helped to maintain the pH stable during the treatment. Moreover, water evaporation from the tap water samples does not entail any significant pH change, thus excluding any possible effect of pH on the observed decrease of DMP degradation efficiency following water evaporation from tap water samples. In addition to pH, the alkalinity caused by carbonate and bicarbonate and the total alkalinity of tap water and evaporated samples were analysed (Table 1). It was observed that the total alkalinity content of the evaporated tap water samples increased from 250 mg $CaCO_3$/L (measured for tap water) to 450 and 740 mg $CaCO_3$/L measured for the concentrated tap water samples with conductivities of 1000 and 2000 µS/cm, respectively. The decrease in DMP degradation efficiency observed with the increase in conductivity of these samples can thus be attributed to scavenging of $^{\bullet}OH$ by carbonate and bicarbonate, as given in Eq. 11 and Eq. 12, respectively (Marotta et al., 2012; Weeks and Rabani, 1966).

$$CO_3^{2-} + \cdot OH \rightarrow CO_3^{\cdot-} + {}^{-}OH \quad k = 4.2x10^8\ M^{-1}s^{-1} \tag{11}$$

$$HCO_3^- + \cdot OH \rightarrow CO_3^{\cdot -} + H_2O \quad k = 8.5x10^6\ M^{-1}s^{-1} \qquad (12)$$

The presence of carbonate and bicarbonate and their negative effect on DMP degradation can also explain the higher DMP degradation rate (i.e. almost twice) in Milli-Q water as compared to tap water.

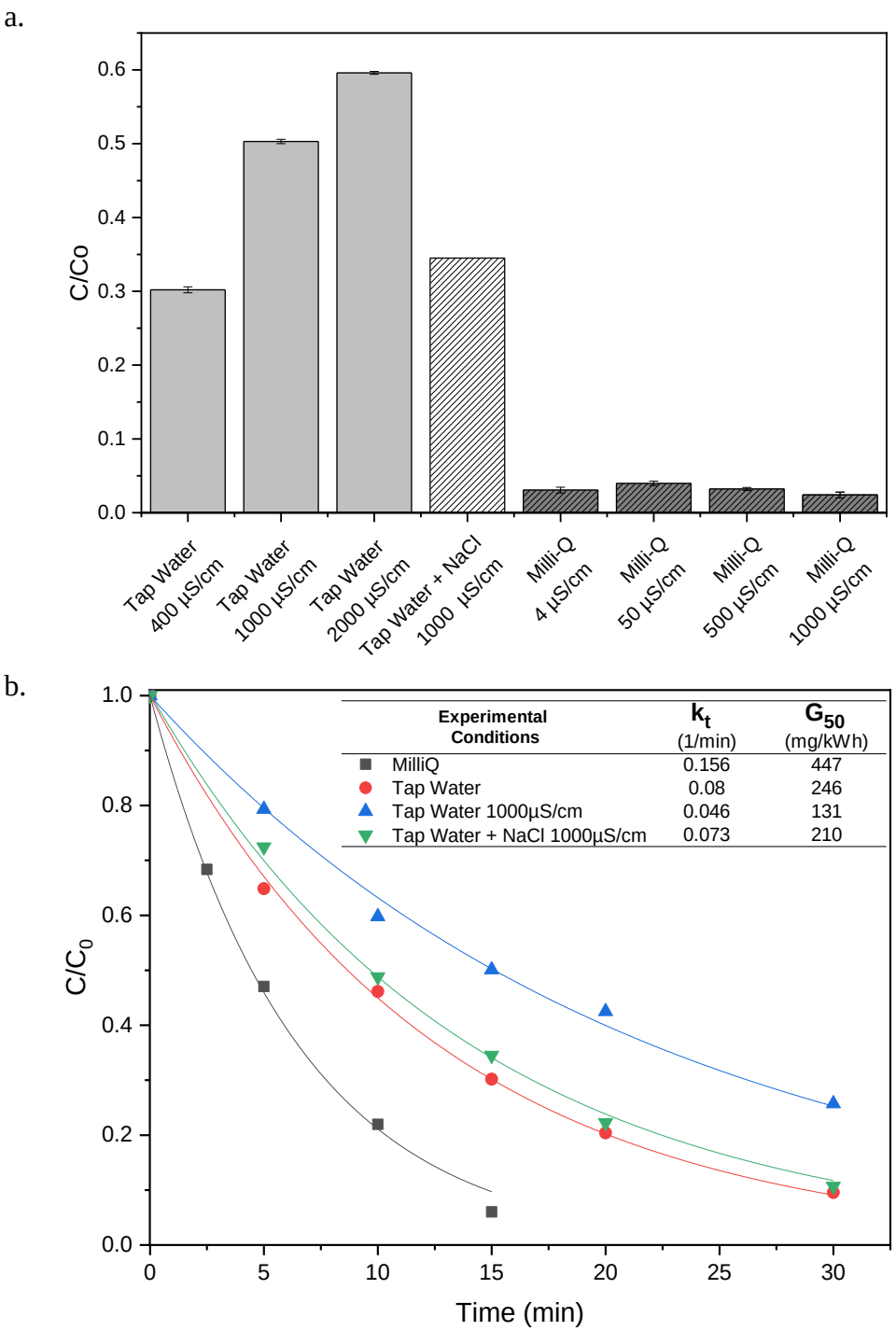

Figure 6 Effect of initial liquid conductivities on **(a)** DMP degradation efficiencies under different solution conditions in tap and Milli-Q water (treatment time = 15 min) **(b)** the DMP degradation efficiencies as a function of treatment time (C_{DMP} = 2x10^{-5} M, P = 3W, DC negative and air).

Table 1. Values of pH and conductivity before and after the degradation of DMP samples in different aqueous media

Sample	pH		Conductivity (µS/cm)		Alkalinity (mg $CaCO_3$/L)		
	Before Treatment	After Treatment	Before Treatment	After Treatment	CO_3^{-2}	HCO_3^-	Total
Milli-Q	6.8	4.8	4.5	42	-	-	-
Tap water	7.8	7.8	430	350	0	250	250
Tap Water 1000 µS/cm	8.2	8.3	990	960	200	250	450
Tap Water 2000 µS/cm	7.7	7.7	1995	1560	440	300	740

Conclusions

The performance of two atmospheric plasma reactors, the SPD and the MCD reactor, was evaluated in the degradation of dimethyl phthalate (DMP) both under air and argon atmosphere. The MCD reactor was the more efficient one achieving almost complete removal of DMP when the pollutant was treated at low initial concentrations using air as plasma gas and applying negative polarity. Analysis of plasma generated reactive species revealed that •OH plays a major role in DMP degradation, followed by O_3. The rate of formation of •OH in the SPD reactor working under argon atmosphere was slightly lower than that in the MCD reactor working in the air. In contrast, however, a significantly higher concentration of hydrogen peroxide accumulated into the solution in the SPD reactor. These observations, which are in apparent contrast, led us to conclude that the SPD reactor, the •OH production rate is probably higher than that measured with the disodium terephthalate probe in the bulk solution. This conclusion seems reasonable considering that SPD in argon produces large amounts of high-energy electrons (Mededovic Thagard et al., 2017; Saleem et al., 2020), which react at the liquid surface, inducing water dissociation to form •OH radicals. Thus, these radicals are present in relatively high local densities at the liquid surface and are quenched thereby fast recombination to form hydrogen peroxide. The latter then diffuses into the bulk solution, reaching relatively high concentrations. This picture is consistent with the results of a previous study in which the SPD reactor proved extremely effective in the degradation of perfluorooctanoic acid (Saleem et al., 2020), a surfactant that accumulates at the liquid surface and reacts with plasma generated species at the water/gas interface. In contrast, when the organic

contaminant has no surfactant properties, as is the case of DMP, SPD does not appear to be particularly convenient for its degradation, which was instead more efficiently achieved in the MCD reactor. This study has also shown that in the MCD reactor the liquid conductivity and the plasma input power have no significant effects on the DMP degradation efficiency, making the MCD reactor suitable for treating liquids with a wide range of initial conductivities. In contrast, carbonate and bicarbonate, known as scavengers of •OH radicals, negatively affected the DMP degradation efficiency.

Acknowledgments

The authors gratefully acknowledge the financial support given by the University of Padova (P-DiSC#06BIRD2019-UNIPD) and the technical support from Mauro Meneghetti and Stefano Mercanzin for the construction of the plasma reactors. Dr.K. Ulucan-Altuntas extend her appreciation to the Scientific and Technological Research Council of Turkey (TUBITAK) with financial support for post-doc research at the University of Padova (Grant Number 1059B191800952).

References

Ahmadi, E., Shokri, B., Mesdaghinia, A., Nabizadeh, R., Reza Khani, M., Yousefzadeh, S., Salehi, M., Yaghmaeian, K., 2020. Synergistic effects of α-Fe2O3-TiO2 and Na2S2O8 on the performance of a non-thermal plasma reactor as a novel catalytic oxidation process for dimethyl phthalate degradation. Separation and Purification Technology 250, 117185. doi:10.1016/j.seppur.2020.117185

APHA, AWWA, W., 2012. Standard Methods for the Examination of Water and Wastewater. twenty-second ed. American Public Health Association, American Water Works Association, Water Environment Federation, Washington 1360.

Arif Malik, M., n.d. Water Purification by Plasmas: Which Reactors are Most Energy Efficient? doi:10.1007/s11090-009-9202-2

Attri, P., Kim, Y.H., Park, D.H., Park, J.H., Hong, Y.J., Uhm, H.S., Kim, K.N., Fridman, A., Choi, E.H., 2015. Generation mechanism of hydroxyl radical species and its lifetime prediction during the plasma-initiated ultraviolet (UV) photolysis. Scientific Reports 5, 1–8. doi:10.1038/srep09332

Bader, H., Hoigné, J., 1981. Determination of ozone in water by the indigo method. Water Research 15, 449–456. doi:10.1016/0043-1354(81)90054-3

Bosi, F.J., Tampieri, F., Marotta, E., Bertani, R., Pavarin, D., Paradisi, C., 2018. Characterisation and comparative evaluation of two atmospheric plasma sources for water treatment. Plasma Processes and Polymers 15, 1700130. doi:10.1002/ppap.201700130

Ceriani, E., Marotta, E., Shapoval, V., Favaro, G., Paradisi, C., 2018. Complete mineralisation of organic pollutants in water by treatment with air non-thermal plasma. Chemical Engineering Journal 337, 567–575. doi:10.1016/j.cej.2017.12.107

Du, C.M., Sun, Y.W., Zhuang, X.F., 2008. The effects of gas composition on active species and byproducts formation in gas-water gliding arc discharge. Plasma Chemistry and Plasma Processing 28, 523–533. doi:10.1007/s11090-008-9143-1

Eisenberg, G.M., 1943. Colorimetric Determination of Hydrogen Peroxide. Industrial and Engineering Chemistry - Analytical Edition 15, 327–328. doi:10.1021/i560117a011

European Union, 1993. Council Regulation (EEC), No. 793/93 of 23 March 1993 on the Evaluation and Control of the Risks of Existing Substances. European Union, Brussels., 1993.

Foster, J.E., 2017. Plasma-based water purification: Challenges and prospects for the future. Physics of Plasmas 24. doi:10.1063/1.4977921

Hsu, P.-C., Kuo, Y.-T., Leon Guo, Y., Chen, J.-R., Tsai, S.-S., Chao, How-Ran; Teng, Y.-N., Pan, M.-H., 2016. The adverse effects of low-dose exposure to Di(2-ethylhexyl) phthalate during adolescence on sperm function in adult rats. Far Eastern Entomologist 165, 16. doi:10.1002/tox

Hu, H., Fang, S., Zhao, M., Jin, H., 2020. Occurrence of phthalic acid esters in sediment samples from East China Sea. Science of the Total Environment 722, 137997. doi:10.1016/j.scitotenv.2020.137997

Jia, H., Cao, Y., Qu, G., Wang, T., Guo, X., Xia, T., 2018. Dimethyl phthalate contaminated soil remediation by dielectric barrier discharge: Performance and residual toxicity. Chemical

Engineering Journal 351, 1076–1084. doi:10.1016/j.cej.2018.06.173

Jiang, B., Zheng, J., Qiu, S., Wu, M., Zhang, Q., Yan, Z., Xue, Q., 2014. Review on electrical discharge plasma technology for wastewater remediation. Chemical Engineering Journal 236, 348–368. doi:10.1016/j.cej.2013.09.090

Kan, H., Wang, T., Yang, Z., Wu, R., Shen, J., Qu, G., Jia, H., 2020. High frequency discharge plasma induced plasticiser elimination in water: Removal performance and residual toxicity. Journal of Hazardous Materials 383, 121185. doi:10.1016/j.jhazmat.2019.121185

Krishna, S., Ceriani, E., Marotta, E., Giardina, A., Špatenka, P., Paradisi, C., 2016. Products and mechanism of verapamil removal in water by air non-thermal plasma treatment. Chemical Engineering Journal 292, 35–41. doi:10.1016/j.cej.2016.01.108

Lee, H., Park, Y.K., Kim, J.S., Park, Y.H., Jung, S.C., 2019. Degradation of dimethyl phthalate using a liquid phase plasma process with TiO2 photocatalysts. Environmental Research 169, 256–260. doi:10.1016/j.envres.2018.11.025

Li, D., Zheng, T., Liu, Y., Hou, D., He, H., Song, H., Zhang, J., Tian, S., Zhang, W., Wang, L., Ma, J., 2020. A cost-effective Electro-Fenton process with graphite felt electrode aeration for degradation of dimethyl phthalate: Enhanced generation of H2O2 and iron recycling that simultaneously regenerates the electrode. Chemical Engineering Journal 394, 125033. doi:10.1016/j.cej.2020.125033

Li, J., Luo, F., Chu, D., Xuan, H., Dai, X., 2017. Complete degradation of dimethyl phthalate by a Comamonas testosterone strain. Journal of Basic Microbiology 57, 941–949. doi:10.1002/jobm.201700296

Liu, Y., Feng, Y., Zhang, Y., Mao, S., Wu, D., Chu, H., 2019a. Highly efficient degradation of dimethyl phthalate from Cu(II) and dimethyl phthalate wastewater by EDTA enhanced ozonation: Performance, intermediates and mechanism. Journal of Hazardous Materials 366, 378–385. doi:10.1016/j.jhazmat.2018.12.003

Liu, Y., Wu, D., Peng, S., Feng, Y., Liu, Z., 2019b. Enhanced mineralisation of dimethyl phthalate by heterogeneous ozonation over nanostructured Cu-Fe-O surfaces: Synergistic effect and radical chain reactions. Separation and Purification Technology 209, 588–597. doi:10.1016/j.seppur.2018.07.016

Locke, B.R., Shih, K.Y., 2011. Review of the methods to form hydrogen peroxide in electrical discharge plasma with liquid water. Plasma Sources Science and Technology 20. doi:10.1088/0963-0252/20/3/034006

Lukes, P., Dolezalova, E., Sisrova, I., Clupek, M., 2014. Aqueous-phase chemistry and bactericidial effects from an air discharge plasma in contact with water: evidence for the formation of peroxynitrite through a pseudo-second-order post-discharge reaction of H2O2 and HNO2. Plasma Sources Science and Technology 23.

Lyche, J.L., Gutleb, A.C., Bergman, Å., Eriksen, G.S., Murk, A.J., Ropstad, E., Saunders, M., Skaare, J.U., 2009. Reproductive and developmental toxicity of phthalates. Journal of Toxicology and Environmental Health - Part B: Critical Reviews 12, 225–249. doi:10.1080/10937400903094091

Mark, G., Tauber, A., Schuchmann, H., Schulz, D., Mues, A., Sonntag, C. Von, 1998. OH-radical formation by ultrasound in aqueous solution – Part II : Terephthalate and Fricke dosimetry and the influence of various conditions on the sonolytic yield. Ultrasonics Sonochemistry 5, 41–52.

Marotta, E., Ceriani, E., Schiorlin, M., Ceretta, C., Paradisi, C., 2012. Comparison of the rates of phenol advanced oxidation in deionised and tap water within a dielectric barrier discharge reactor. Water Research 46, 6239–6246. doi:10.1016/j.watres.2012.08.022

Marotta, E., Schiorlin, M., Ren, X., Rea, M., Paradisi, C., 2011. Advanced oxidation process for degradation of aqueous phenol in a dielectric barrier discharge reactor. Plasma Processes and Polymers 8, 867–875. doi:10.1002/ppap.201100036

Mededovic Thagard, S., Stratton, G.R., Dai, F., Bellona, C.L., Holsen, T.M., Bohl, D.G., Paek, E., Dickenson, E.R.V., 2017. Plasma-based water treatment: Development of a general mechanistic model to estimate the treatability of different types of contaminants. Journal of Physics D: Applied Physics 50. doi:10.1088/1361-6463/50/1/014003

Miichi, T., Kanzawa, R., 2018. Advanced Oxidation Process using DC Corona Discharge over Water. Electronics and Communications in Japan 101, 65–72. doi:10.1002/ecj.12064

Moreno, J.D., Rodríguez S, J.L., Poznyak, T., Chairez, I., Dorantes-Rosales, H.J., 2020. Effect of the type of soil on dimethyl phthalate degradation by ozone. Journal of Environmental Management 270. doi:10.1016/j.jenvman.2020.110863

Nani, L., Tampieri, F., Ceriani, E., Marotta, E., Paradisi, C., 2018. ROS production and removal of the herbicide metolachlor by air non-thermal plasma produced by DBD, DC- and DC+ discharges implemented within the same reactor. Journal of Physics D: Applied Physics 51. doi:10.1088/1361-6463/aab8b9

Qi, Z.H., Yang, L., Xia, Y., Ding, Z.F., Niu, J.H., Liu, D.P., Zhao, Y., Ji, L.F., Song, Y., Lin, X.S., 2019. Removal of dimethyl phthalate in water by non-thermal air plasma treatment. Environmental Science: Water Research and Technology 5, 920–930. doi:10.1039/c9ew00072k

Sahni, M., Locke, B.R., 2006. Quantification of hydroxyl radicals produced in aqueous phase pulsed electrical discharge reactors. Industrial and Engineering Chemistry Research 45, 5819–5825. doi:10.1021/ie0601504

Saleem, M., Biondo, O., Sretenović, G., Tomei, G., Magarotto, M., Pavarin, D., Marotta, E., Paradisi, C., 2020. Comparative performance assessment of plasma reactors for the treatment of PFOA; reactor design, kinetics, mineralisation and energy yield. Chemical Engineering Journal 382, 123031. doi:10.1016/j.cej.2019.123031

Shiraki, D., Ishibashi, N., Takeuchi, N., 2016. Quantitative Estimation of OH Radicals Reacting in Liquid Using a Chemical Probe for Plasma in Contact With Liquid 44, 3158–3163.

Slater, R.C., Douglas-Hamilton, D.H., 1981. Electron-beam-initiated destruction of low concentrations of vinyl chloride in carrier gases. Journal of Applied Physics 52, 5820–5828. doi:10.1063/1.329476

Sretenović, G.B., Saleem, M., Biondo, O., Tomei, G., Marotta, E., 2021. Spectroscopic study of self-pulsing discharge with liquid electrode Spectroscopic study of self-pulsing discharge with liquid electrode 183308. doi:10.1063/5.0044331

Stratton, G.R., Dai, F., Bellona, C.L., Holsen, T.M., Dickenson, E.R.V., Mededovic Thagard, S., 2017. Plasma-Based Water Treatment: Efficient Transformation of Perfluoroalkyl Substances in Prepared Solutions and Contaminated Groundwater. Environmental Science and Technology 51, 1643–1648. doi:10.1021/acs.est.6b04215

Tampieri, F., Giardina, A., Bosi, F.J., Pavanello, A., Marotta, E., Zaniol, B., Neretti, G., Paradisi,

C., 2018. Removal of persistent organic pollutants from water using a newly developed atmospheric plasma reactor. Plasma Processes and Polymers 15. doi:10.1002/ppap.201700207

Tarabova, B., Lukes, P., Janda, M., Hensel, K., Sikurova, L., Machala, Z., 2018. Specificity of detection methods of nitrites and ozone in aqueous solutions activated by air plasma. Plasma Processes and Polymers 15.

US EPA, National Primary Drinking Water Regulations, Federal Register; 40 CFR Chapter I, Part 141. US Environmental Protection Agency, Washington, DC, 1991. 663–664.

Wang, F., Yao, J., Sun, K., Xing, B., 2010. Adsorption of dialkyl phthalate esters on carbon nanotubes. Environmental Science and Technology 44, 6985–6991. doi:10.1021/es101326j

Wang, T., Jia, H., Guo, X., Xia, T., Qu, G., Sun, Q., Yin, X., 2018a. Evaluation of the potential of dimethyl phthalate degradation in aqueous using sodium percarbonate activated by discharge plasma. Chemical Engineering Journal 346, 65–76. doi:10.1016/j.cej.2018.04.024

Wang, T., Qu, G., Yin, X., Sun, Q., Liang, D., Guo, X., Jia, H., 2018b. Dimethyl phthalate elimination from micro-polluted source water by surface discharge plasma: Performance, active species roles and mechanisms. Journal of Hazardous Materials 357, 279–288. doi:10.1016/j.jhazmat.2018.06.014

Wang, X., Wang, P., Liu, X., Hu, L., Wang, Q., Xu, P., Zhang, G., 2020. Enhanced degradation of PFOA in water by dielectric barrier discharge plasma in a coaxial cylindrical structure with the assistance of peroxymonosulfate. Chemical Engineering Journal 389, 124381. doi:10.1016/j.cej.2020.124381

Weeks, J.L., Rabani, J., 1966. The pulse radiolysis of deaerated aqueous carbonate solutions. I. Transient optical spectrum and mechanism. II. pK for OH radicals. Journal of Physical Chemistry 70, 2100–2106. doi:10.1021/j100879a005

Xu, Z., Xiong, X., Zhao, Y., Xiang, W., Wu, C., 2020. Pollutants delivered every day: Phthalates in plastic express packaging bags and their leaching potential. Journal of Hazardous Materials 384, 121282. doi:10.1016/j.jhazmat.2019.121282

Yang, F., Liu, X.H., He, W., Xiao, H.G., 2013. Investigation on characteristics of argon corona discharge under atmospheric pressure. Indian Journal of Physics 87, 391–400. doi:10.1007/s12648-012-0238-4

Zhang, T., Huang, Z., Chen, X., Huang, M., Ruan, J., 2016. Degradation behavior of dimethyl phthalate in an anaerobic/anoxic/oxic system. Journal of Environmental Management 184, 281–288. doi:10.1016/j.jenvman.2016.10.008

Zhao, H., Wang, Q., Chen, Y., Tian, Q., Zhao, G., 2017. Efficient removal of dimethyl phthalate with activated iron-doped carbon aerogel through an integrated adsorption and electro-Fenton oxidation process. Carbon 124, 111–122. doi:10.1016/j.carbon.2017.08.034

Zhao, X., Shen, J. min, Zhang, H., Li, X., Chen, Z. lin, Wang, X. chun, 2020. The occurrence and spatial distribution of phthalate esters (PAEs) in the Lanzhou section of the Yellow River. Environmental Science and Pollution Research 27, 19724–19735. doi:10.1007/s11356-020-08443-7